Spin waves in circular soft magnetic dots at the crossover between vortex and single domain state

Farkhad G. Aliev,[1,*] Juan F. Sierra,[1] Ahmad A. Awad,[1] Gleb N. Kakazei,[2,†] Dong-Soo Han,[3] Sang-Koog Kim,[3] Vitali Metlushko,[4] Bojan Ilic,[5] and Konstantin Y. Guslienko[3,6]

[1]*Departamento de Fisica de la Materia Condensada, CIII, Instituto "Nicolas Cabrera" de Ciencia de Materiales, Universidad Autonoma de Madrid, 28049 Madrid, Spain*

[2]*Departamento de Física da Faculdade de Ciências, IFIMUP and IN-Institute of Nanoscience and Nanotechnology, Universidade do Porto, 4169-007 Porto, Portugal*

[3]*Research Center for Spin Dynamics and Spin-Wave Devices, Seoul National University, Seoul, 1510744 South Korea*

[4]*Department of Electrical and Computer Engineering, University of Illinois at Chicago, Chicago, Illinois, 60607 USA*

[5]*Cornell Nanofabrication Facility, Cornell University, Ithaca, New York, 14853 USA*

[6]*Departamento de Fisica de Materiales, Universidad del Pais Vasco, 20018 Donostia-San Sebastian, Spain*

(Received 21 April 2009; published 28 May 2009)

We report on linear spin dynamics in the vortex state of Permalloy cylindrical dots subjected to an in-plane bias magnetic field. We demonstrate experimentally by a broadband ferromagnetic resonance technique and by simulations that breaking the cylindrical symmetry of the magnetic vortex gradually changes and suppresses the azimuthal spin eigenmodes below the vortex nucleation field and leads further to the appearance of new eigenmodes. The parallel microwave field pumping is shown to be a unique tool to observe spin excitation modes localized near the strongly shifted vortex core for the bias field between the vortex nucleation and annihilation fields. Meanwhile, the perpendicular field pumping, which excites the spin waves throughout the entire dot, reveals a crossover between two dynamic vortex regimes near the nucleation field.

DOI: 10.1103/PhysRevB.79.174433 PACS number(s): 75.40.Gb, 75.40.Mg, 75.75.+a, 76.50.+g

In many physical systems such as liquids, plasma, superconductors, ferromagnets, etc., the topological excitations (vortices) are frequently subjected to stratified conditions breaking the axial symmetry.[1,2] The special interest in confined magnetic vortices[3] is inspired by the possibility of switching the vortex core direction[4] in magnetic dots that has been suggested as a potential new route to create nanoscale magnetic memory units. A precise mapping of the high-frequency spin excitation eigenmodes, *especially the eigenmodes breaking axial symmetry*, is of great importance because these modes are expected to define the vortex switching characteristic times and routes to reduce the critical currents for magnetoelectronic nanostructures operating under magnetic field.

It is known that without a bias field multiple spin eigenmodes can be excited in the magnetic vortex state by an external perturbation and the dynamical response in the linear regime is described by their superposition. The lowest frequency excitation corresponds to the gyrotropic mode, when the vortex moves as a whole around an equilibrium position,[5–7] while the higher frequency modes correspond to spin waves excited mainly outside of the vortex core.[8–17] The spin waves having radial or azimuthal symmetry with respect to the dot center are described by integers (n,m), which indicate the number of nodes of the dynamic magnetization components $\propto \sin(m\varphi-\omega t)$, $\cos(m\varphi-\omega t)$ along the radial (n) and azimuthal (m) directions (φ is the azimuthal angle in the dot plane and ω is the spin-wave frequency). The spin-wave eigenfrequencies $\omega_{n,m}$ are quantized due to strong pinning boundary conditions on the dot lateral edges.[3] With an in-plane magnetic excitation field the azimuthal spin waves having $m=\pm 1$ and the gyrotropic mode are expected to be excited[13,16,17] because only these spin modes have nonzero average in-plane magnetization and can interact with the uniform rf driving field. Previous investigations were mainly focused on spin waves in the absence of bias magnetic field,[6–9,11,12,14,15] with the vortex localized in the dot center. In particular, the zero-field splitting of the azimuthal spin-wave mode frequencies was observed in Refs. 6 and 13.

Initial studies of the spin waves in the vortex state under the influence of an in-plane bias field were conducted in Refs. 16 and 17. Broadband vector network analyzer ferromagnetic resonance (VNA-FMR) results in applied magnetic field were reported for circular dots with a big aspect ratio (the dot thickness L to radius R ratio was $L/R=0.15$) in Ref. 16, where up to eight modes were observed in the vortex state. Then Neudecker *et al.*[17] investigated dots with a large diameter (4 μm) and very small aspect ratio ($L/R=0.01$). Two excitation modes were observed up to vortex annihilation field $H<H_a$ by ferromagnetic resonance scanning Kerr microscopy (FMR-SKEM) and it was found that the low-frequency spin mode transforms to the Kittel's mode increasing the bias field. The FMR-SKEM optic technique allows getting spatial images of the dynamic magnetization distributions, but it is only applicable (i) to large in-plane size dots (near the border of the single vortex-state stability) because the light spot must be much smaller than the dot diameter and (ii) only to few low-frequency spin-wave modes, which have a relatively small number of nodes of the dynamical magnetization. The spatial resolution of optic probes (>300 nm, Ref. 17) is not sufficient for a clear spatiotemporal observation of all the excited modes in dots with diameter of about 1 μm and below. Applying the VNA-FMR technique, Neudecker *et al.*[17] observed just one spin-wave mode due to the dense mode spectrum and insufficient frequency resolution for such thin large-diameter dots [the in-

termode separation is proportional to $(L/R)^{1/2}$]. For instance, they were unable to resolve the zero-field splitting of the azimuthal modes, which being proportional to L/R is very small (0.15 GHz) and is beyond their experimental resolution of about 0.5 GHz. We also note that the authors of Refs. 16 and 17 never used parallel pumping scheme, which is the most effective method to excite the spin modes in the vortex state. The VNA-FMR results[16,17] therefore are not sufficient to understand the real field-dependent spin-wave spectra of the biased vortex dots. The FMR-SKEM results obtained for a very special case in Ref. 17 cannot be generalized to describe smaller dots due to the absence of scaling of the spin eigenfrequencies when decreasing the in-plane dot sizes. Other existing technique, namely, x-ray imaging based on the magnetic circular dichroism effect,[4] has a sufficient spatial resolution, but is not fast enough to resolve the spin-wave modes with frequencies about 5–10 GHz and is currently employed only to detect the low-frequency gyrotropic vortex modes (100 MHz frequency range).

Summarizing the introduction part, despite of a huge current interest in the manipulation of the gyrotropic mode in the centered (unshifted) vortex ground state, there is little understanding concerning the spin waves excited in a strongly shifted nonuniform magnetic vortex state. This unexplored regime, however, is not only of fundamental interest, but is also of great importance for potential applications in magnetic recording and spintronics. For instance, a precise knowledge of the spin-wave modes in the biased vortex state is crucial for the spin-polarized current-induced switching of the free layer in nanopillar devices. Our article describes the spin dynamics in the strongly nonuniform (vortex) asymmetric state of magnetic dots with a moderate aspect ratio $L/R \sim 0.05-0.1$, which could be generalized to smaller and larger dots.

We report on precise broadband measurements and simulations of the vortex dynamics in circular Permalloy (Py) dots excited by applying an in-plane driving field with different angles between the bias and excitation fields. We present the measured variation of spin-wave frequencies vs bias field in a wide field region covering the vortex and saturated states. We show that independently of the rf pumping orientation the azimuthal modes survive only below the vortex nucleation field. With parallel rf pumping we identify an unexpected spin-wave eigenmode in the weakly shifted vortex state and a spin-wave mode localized near the strongly shifted vortex core, which was recently discussed in Ref. 18. These modes can be only excited by parallel pumping and exist only in the magnetic vortex state shifted from the dot center. With perpendicular pumping, which excites modes in the entire Py dot, we clearly observed a crossover in the spin-wave dynamics of the shifted vortex near the vortex nucleation field.

We report below on three observations:

(1) We show that contrary to the previously reported results,[16,17] the spin-wave modes with azimuthal symmetry (having nonzero azimuthal indices m) do not survive up to the vortex annihilation field. They transform to other kinds of spin-wave modes when the bias magnetic field shifts the vortex core from the dot center.

(2) We identify a specific spin-wave mode localized near the shifted vortex core (mode 3 in Fig. 1) in relatively high magnetic fields.

(3) We present an observation of fundamental differences in the field dependences of the spin-wave spectra excited with perpendicular and parallel pumping.

These extensive dynamic measurements and simulations allow us to present the spin-wave response of the shifted magnetic vortex state in three-dimensional (3D) plots, providing a clear frame for unambiguous identification of the spin-wave excitation spectrum. The main finding of our work, however, is not just the observation of the differences between spin-wave modes excited with the parallel and perpendicular pumping schemes, but also that these modes transform in a fundamentally different way when the magnetic vortex is displaced by the in-plane bias field.

Two sets of square arrays of Py circular dots were fabricated by combination of lithography and lift-off techniques on a standard Si(100) substrate as explained elsewhere.[13,19,20] The first set includes three samples with thickness $L=50$ nm, diameter $D=1000$ nm, and lattice parameters of the dots (center-to-center distance, cc) of 1200, 1500, and 2500 nm. The second set included two arrays of Py dots with thickness $L=25$ nm and diameters of $D=1035$ nm ($cc=2000$ nm) and of 572 nm ($cc=1000$ nm). The excited spin waves have been studied at room temperature with a broadband spectrometer based on a vector network analyzer (VNA).[21] The setup allows to apply a rf field either in perpendicular configuration ($\mathbf{h}_{\mathrm{rf}\perp}$), where $\mathbf{H}_{\mathrm{bias}} \| \mathbf{x}$ and $\mathbf{h}_{\mathrm{rf}} \perp \mathbf{x}$ as shown in Fig. 1(a), or with a parallel pumping scheme ($\mathbf{h}_{\mathrm{rf}\|}$), when $\mathbf{H}_{\mathrm{bias}} \| \mathbf{x}$ and the coplanar wave guide (CPW) is rotated perpendicularly with respect to the in-plane static bias field, providing $\mathbf{h}_{\mathrm{rf}} \| \mathbf{x}$. Data were analyzed on the basis of the transmission model developed under the assumption that the dominant CPW mode is the TEM mode and also neglecting the effect of reflection.[14] The estimated magnitude of the in-plane rf field is below 0.2 Oe.

Besides the experimental VNA-FMR studies, extensive micromagnetic simulations[22] were carried out for a circular Py dot having a thickness of 25 nm and a diameter of 1035 nm. The physical parameters of the individual cells of $5 \times 5 \times 25$ nm^3 used were the exchange stiffness constant $A = 1.4 \times 10^{-11}$ (J/m), the saturation magnetization $M_s = 830 \times 10^3$ A/m, the gyromagnetic ratio $\gamma/2\pi = 2.96$ MHz/Oe taken from the measurements,[19] and the Gilbert damping constant of $\alpha = 0.01$.

We first identify the vortex nucleation (H_n) and annihilation (H_a) fields for the dots having the vortex remanent state. These fields approximately describe a range of field stability of the vortex ground state.[8] Figure 1(b) shows the typical dependence of the normalized magnetization ($\boldsymbol{M}$) on the in-plane magnetic field during the hysteresis cycle for the positive field branch with H_n and H_a fields marked by vertical arrows. In order to compare the static and dynamic measurements we normalized the bias field by H_a. To study experimentally the vortex ground-state excitations we first saturated $\boldsymbol{M}$ by the in-plane magnetic field (H) above the annihilation field ($H > 3H_a$). Then, the magnetic field was swept within the interval $-3H_a < H < 3H_a$ creating and annihilating the vortex state. We present here the experiments [Figs. 1(c) and 1(d)] and simulations [Figs. 2(a) and 2(b)] of

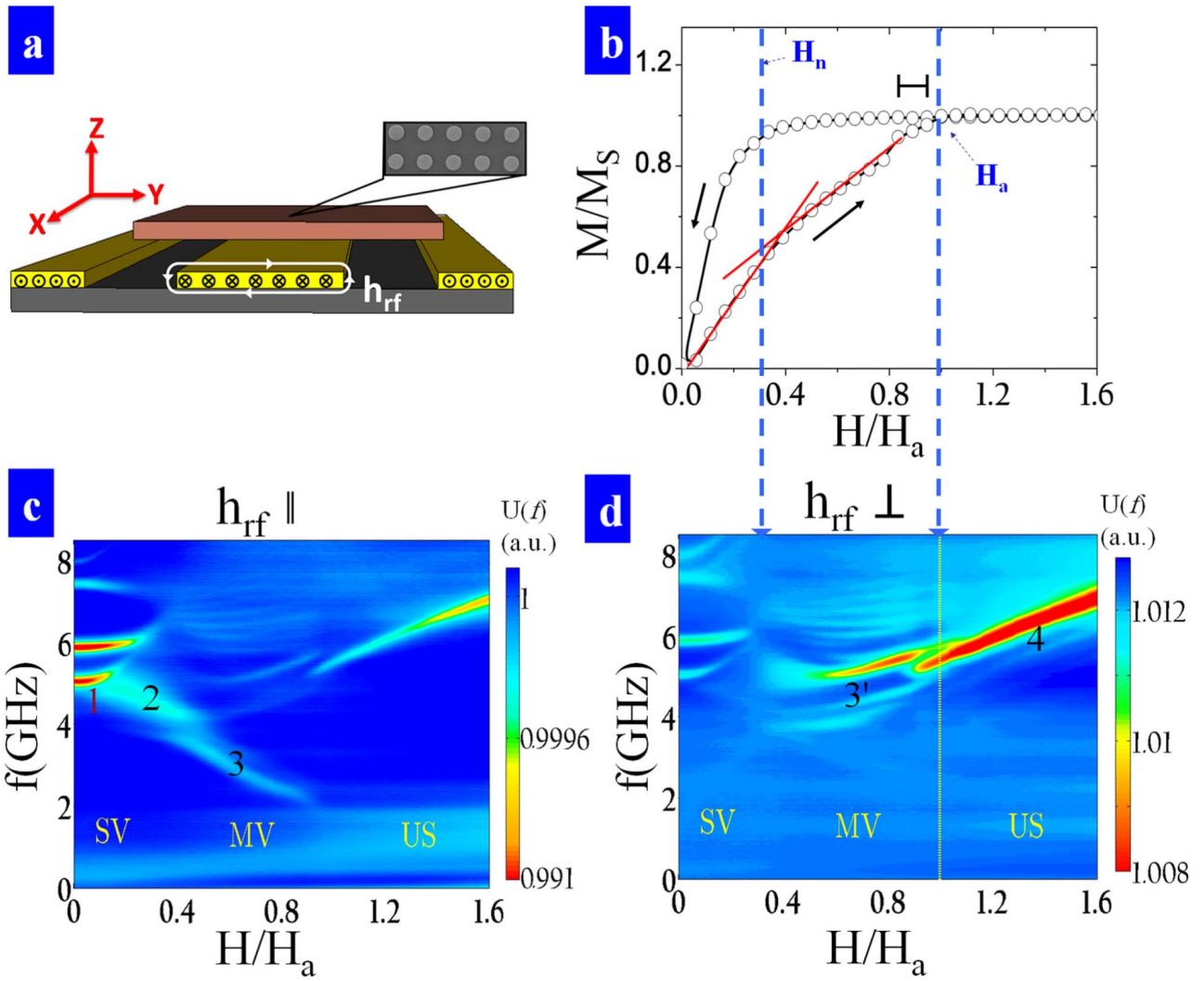

FIG. 1. (Color online) (a) Sketch of the experimental setup and the coordinate system used. Insert shows a typical SEM image of an array of Py dots. The bias magnetic field is directed along the x or y axes. (b) Magnetization vs magnetic field normalized by the vortex annihilation field (H_a=360 Oe). Vertical dashed lines indicate the vortex nucleation and annihilations fields, while the error bar evaluates the uncertainty in vortex annihilation field. Red lines indicate the change in the slope of the $M(H)$ dependence near H_n. [(c) and (d)] Intensity plots of the measured spin-wave spectra for the Py dot arrays with thickness 25 nm and 1035 nm diameter for the driving rf field (c) parallel and (d) perpendicular to the increasing bias magnetic field. Numbers 1, 2, 3, 3′, and 4 label the spin-wave eigenmodes discussed in the text.

spin dynamics in Py dots with thickness of 25 nm and diameter of 1035 nm by using either parallel ($\mathbf{h}_{\mathrm{rf}\parallel}$) or perpendicular ($\mathbf{h}_{\mathrm{rf}\perp}$) rf drive and observed with increasing bias field from zero to above the annihilation field. Similar results have been also obtained for other dot arrays with the aspect ratio thickness/radius (L/R) varied between 0.05 and 0.1 revealing extra higher frequency modes appearing in the measured spectral window for smaller values of L/R. The dynamic response remains qualitatively unaffected by the interdot dipole-dipole interaction with more than a twofold change in the interdot distance ensuring that we are observing single dot eigenmodes.

Let us first discuss the experimental results [Figs. 1(c) and 1(d)]. Applying the uniform rf field $\mathbf{h}_{\mathrm{rf}}$ we excite only the spin eigenmodes localized in the areas where the torque $\mathbf{h} \times \mathbf{M}_0 \neq 0$ ($\mathbf{M}_0$ is the static dot magnetization). In the small field regime $H < H_n$ (further stable vortex, SV) two doublets of the spin eigenmodes are observed with the eigenfrequencies being independent of the orientation of the rf field [see Figs. 1(c) and 1(d)]. These low-field doublets can be described[23] as azimuthal spin waves with the indices $n=0$, $m=\pm 1$ indicated in Fig. 1 as (1) and with the indices $n=1$, $m=1$; $n=0$, $m=0$. The latter modes have much lower intensity and will not be discussed further. The observed zero-field splitting of the spin eigenfrequencies of the doublets $n=0$, $m=\pm 1$ is about 1 GHz in accordance with a recently developed model[23] of the dynamical vortex core–azimuthal spin-wave interaction.

We note that previous works[16,17] described data in terms of azimuthal spin-wave modes with the indices (n,m) as unchanged between the cylindrical (zero field) and fully broken (near the vortex annihilation field) symmetries of the magnetization ground state. However, this assumption obviously has no sense from the symmetrical point of view and interpretation of these modes and the mode indices should be corrected because the azimuthal modes cannot survive up to

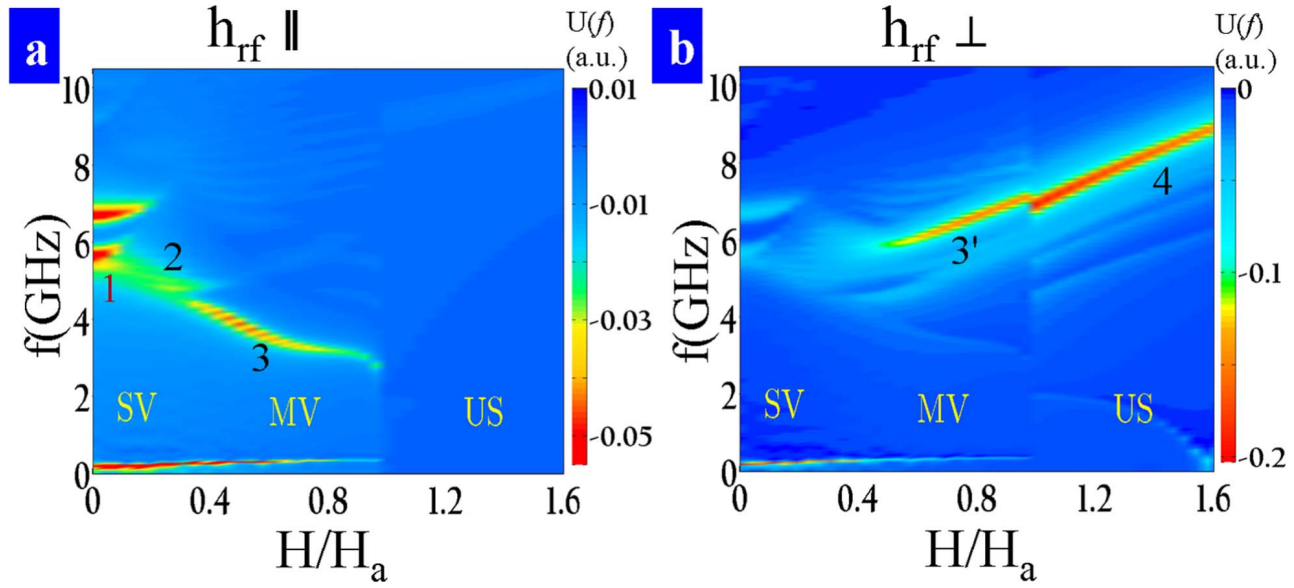

FIG. 2. (Color online) Intensity plots of the simulated spectra for the Py dot arrays with thickness 25 nm and 1035 nm diameter for rf field (a) parallel and (b) perpendicular to the increasing bias magnetic field. Numbers 1, 2, 3, 3′, and 4 label the spin-wave modes discussed in the text.

the vortex annihilation field. The spin-wave eigenmode's (n,m) classification is strictly applicable to the zero-field case. Neudecker *et al.*[16,17] assumed that the modes keep their indices having sense only for cylindrical symmetry $(H=0)$ for the entire field region, up to the annihilation field, H_a. However, our experiments show that they can be approximately used only up to $H \approx H_n$. At small H one can excite the spin eigenmodes with indices $m=0, \pm 2$, whose intensities are proportional to H^2. The first mode is not observed in our simulations (see below), whereas the $m=\pm 2$ $(n=0)$ modes are responsible for the formation of the spin-wave branch (2) observed with parallel pumping. The fundamental importance of the parallel pumping[18] is that it excites only the modes localized close to the strongly shifted vortex core. We note that the spin-wave mode localization discussed here is a result of the nonuniform ground state, whereas the mode localization at the dot edges discussed in Ref. 24 is due to a nonuniform internal field for quasiuniformly magnetized dots. When the vortex core is sufficiently shifted from the center of the disk (further metastable vortex, MV), there is an essential area of the dot, where the static magnetization $\mathbf{M}_0$ is parallel to the bias field $\mathbf{H}$. Therefore, the parallel pumping excites only modes near the vortex core. This is contrary to the usually employed perpendicular pumping scheme, which provides a much broader spin-wave spectrum because the microwave field is strongly coupled to different spin eigenmodes throughout the sample. This explains the importance of the parallel pumping to provide information on the spin-wave modes localized near the vortex core (mode n.3). We observed that the "soft" mode (3) exists also only with parallel pumping when the vortex core is close to the dot edge at $H_n < H < H_a$.

Increasing the bias field with the perpendicular pumping also suppresses the azimuthal modes $|m|=1$ at $H > H_n$. The perpendicular pumping scheme in the strongly shifted vortex state provides a much broader (than parallel pumping) spin-wave spectrum because the microwave driving field is strongly coupled to different modes throughout the sample. Increasing H with $\mathbf{h}_{\mathrm{rf}\perp}$ reveals a crossover between three main field regions in the excitation spectra: from SV state $(H < H_n)$, where the eigenmodes classification is still applicable, to the strongly shifted (MV state) with a much broader spin-wave spectrum and, finally, to the quasi-uniform or saturated state (US). There are two energy minima in the MV field region, corresponding to shifted vortex and quasi-uniform magnetization states.[25] It is important to underline that the parallel or perpendicular pumping field can excite fundamentally different spin modes in the MV state $(H_n < H < H_a)$. Indeed, the frequency of the localized near vortex core mode (3) observed for the MV with the $\mathbf{h}_{\mathrm{rf}\parallel}$ configuration [see Fig. 1(b)] decreases with increasing magnetic field. In contrast, using $\mathbf{h}_{\mathrm{rf}\perp}$ in the MV state excites a dominant paraboliclike mode marked as (3′), accompanied by multiple satellites [Fig. 1(d)], which transforms abruptly near the annihilation field H_a into the almost uniform precession mode (4) existing at $H > H_a$ in the US. Only edge modes are excited with the parallel pumping in the US. [Fig. 1(b)]. Figure 1 shows more clearly other fundamental differences of the detected spectra for parallel (part c) and perpendicular (part d) rf excitations. While for the parallel excitation both the azimuthal modes merge close to the vortex nucleation field with a new mode (2) excited at the transition between the stable and metastable vortex states, the field dependence of the modes excited with perpendicular pumping is very different. One clearly sees a vertical zone (marked by the vertical dashed arrow) presented in the dynamic response close to the vortex nucleation field, with no modes excited. Measurements conducted in this specific field range between the stable and metastable vortex states clearly show that the spin-wave modes excited with perpendicular pumping in the MV state (such as the mode 3′) do not represent a continuous transformation of those modes excited in the symmetri-

cal (almost symmetrical) vortex ground state ($H<H_n$). We note that in Ref. 17 only one mode was found by VNA-FMR with perpendicular pumping and the indices ($n=0$, $m=1$, our notations) were assigned to it for the entire field region from zero to the field well above H_a, whereas we clearly established that there are at least four intensive azimuthal modes with the indices $n=0$, $m=+1/-1$, and $n=1$, $m=+1/-1$ having a significant frequency splitting. All the modes exist only below H_n.

An analysis of the linewidth of the spin-wave modes presented in Fig. 1 reveals that the lowest ($n=0;m=\pm 1$) azimuthal modes observed in small magnetic fields are characterized by a relatively narrow linewidth of about 250 ± 50 MHz being almost field independent in the SV state. The observed linewidth for both the pumping schemes is close to the one measured in the uniform state near the border between the MV and US states. The spin-wave modes (2), (3), and (3′) detected in the MV state are characterized, however, by much a broader linewidth of about 800 ± 300 MHz, with the error bar attributed to weaker signals. The mode (2) linewidth reveals a maximum at H_n (parallel pumping), whereas the mode (3′) linewidth reaches its maximum values just below H_{an}. We note that qualitatively different results were reported in Ref. 17 for perpendicular pumping, where the sharp maximum in the VNA-FMR linewidth of the single observed mode (interpreted as the first azimuthal mode with $n=0$, $m=1$) as a function of magnetic field was observed between H_n and H_{an} in the vortex state and was attributed to possible variations in the dots dimensions and to the integrative nature of the VNA-FMR technique.

To understand in detail the excited spin eigenmodes in the frequency domain at a given bias field, we conducted the micromagnetic simulations by applying the field to the vortex-state dot along the x direction in the range from 0 to 1000 Oe with steps of 20 Oe. Our numerical results provide an annihilation field of 500 Oe. The difference with the experimentally measured value could be due to the weak dipolar coupling between the dots and to the fact that the simulations are done at $T=0$ K. Both the $\mathbf{h}_{\mathrm{rf}\parallel}$ and $\mathbf{h}_{\mathrm{rf}\perp}$ pumping schemes were explored by applying a sine field of variable frequency and with an amplitude of 1 Oe. Figure 2 shows the simulated Fourier power spectra in a wide frequency range as a function of the bias field normalized by H_a for parallel (part a) and perpendicular (part b) pumping schemes, which are in rather good agreement with experiments [Figs. 1(c) and 1(d)]. Figure 3 shows simulated spatial distributions of the dynamic magnetization in the parallel ($\Delta M_x/M_s$) and the perpendicular ($\Delta M_y/M_s$) pumping schemes for the most intensive excited modes (marked as 1–4 in Figs. 1 and 2) at some specific frequencies and normalized fields. The lowest ($n=0,m=+1$) azimuthal mode (1) is observed in zero-bias field. The application of a weak field (e.g., $H/H_a=0.077$) smoothly breaks the vortex-state cylindrical symmetry but maintains the character of the mode (1). As pointed above, the mode (2) splitting out from the lowest azimuthal mode *has a qualitatively character* described approximately as a superposition of the azimuthal spin-wave modes $m=\pm 2$ rotating around the vortex core in the opposite directions (clockwise, CW and counterclockwise, CCW). Given the vortex core shift in the positive y direction, the modes start from the positive y semi-axis, propagate, meet each other, and disappear at the negative y semi-axis. When the bias field is further increased (4.86 GHz, $H/H_a=0.423$), the mode (2) also shows a similar motion but with more nodes in the disturbed azimuthal direction (Fig. 3). We can distinguish two different regions in the dynamical $\boldsymbol{M}$ images. In the first one, close to the vortex core, there is a superposition of the CCW and CW motions. In the second region (far from the vortex core, the lower part of the dot) *standinglike spin-wave modes dominate* (Fig. 3, mode 2, $f=\omega/2\pi=4.86$ GHz). The increase of the bias field expands the second region. On the other hand, there is a clear standing whiskerlike dominating pattern for the lower frequency mode [mode (3), 4.18 GHz, MV]. These modes are localized near the deformed vortex core (where the static magnetization component M_y has a significant value) and the reduced area occupied by the modes gradually decreases with increasing of the bias field (compare the images for $H/H_a=0.423$ and 0.923 in Fig. 3). This spin mode (3) can be approximately described for low fields (just around H_n) as having a wave vector along the bias field $\mathbf{H}$ (analogy to the backward volume magnetostatic spin waves in continuous films) because the nodal planes are perpendicular to the x direction.

When we applied the perpendicular drive, the response in the low-field region (SV) is the same as in the parallel case. In the MV region the high-frequency mode (3′) is more intensively excited compared to the parallel pumping case [mode (3)]. Mode (3′) is localized mainly outside the vortex core in the domain magnetized parallel to the bias field. In general, mode (3′) dynamic $\mathbf{M}$ images are similar to those observed for mode (3) for weaker fields in the MV state (5.84 GHz, 0.423), but become more complicated close to the boundary with the US increasing the bias field (6.88 GHz, 0.923). We note that the transition to the US regime suppresses abruptly the (3) mode, but the quasi-uniform Kittel-type mode (4) is a continuation of the (3′) mode, not of the ($n=0,m=1$) azimuthal mode as stated in Ref. 17. For complete sequences of the data shown in Fig. 3, see movies in Ref. 26. We attribute the small (<10%) disagreement between the experimental and simulated spin eigenmodes to (i) an influence of the interdot dipolar interaction (ii) the presence of a small out-of-plane rf component (Fig. 1), and (iii) to the thin (about 2 nm) Py oxide layer[27] which influences the dot thickness and, therefore, the spin eigenfrequencies.[8]

In conclusion, the spin-wave eigenmodes (n,m) classification based on the number of nodes in radial and azimuthal directions could be applicable to the vortex shifted by magnetic field only below the vortex nucleation field. Microwave excitation in different directions with respect to the bias field reveals a unique information on spin-wave dynamics in the strongly shifted vortex state, particularly on the modes localized near the vortex core. Our results are important for understanding the dynamics in different vortex systems in confined biased conditions, e.g., in arrays of vortex nano-oscillators excited by a spin-polarized current.[28] The perpendicular and parallel excitation schemes do not just reflect the coupling of rf field to the different modes, but what is more critical, the excited spin-wave mode frequencies vary in qualitatively different way as the vortex is shifted from the

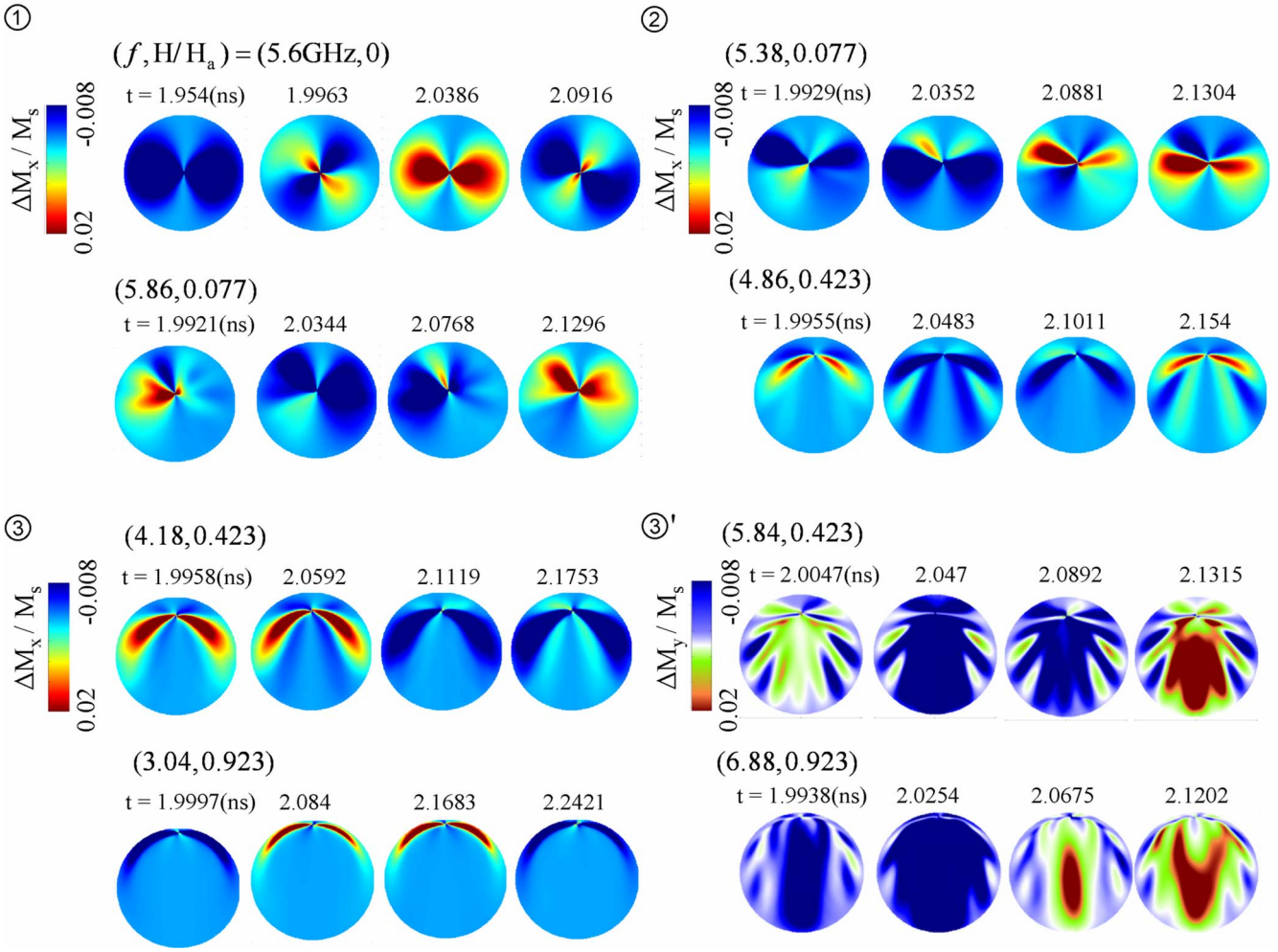

FIG. 3. (Color online) Simulated (in the form of time sequences with a step of about $\frac{1}{4}$ oscillation period) spatial distributions of the vortex dynamic magnetization in the SV and MV field regions. Numbers 1, 2, and 3 denote the spin-wave eigenfrequency branches for parallel pumping (the magnetization component $\Delta M_x/M_s$) and 3′ for perpendicular pumping (the component $\Delta M_y/M_s$) in Figs. 1 and 2. The first number in brackets $(f, H/H_a)$ shows the eigenmode frequency, whereas the second number shows the normalized magnetic bias field. The images are selected for the frequency/field points where splitting of the eigenfrequencies occurs at each frequency branch.

dot center to the dot edge for the parallel and perpendicular excitations. The insights into the spin-wave dynamics in the magnetic vortex state presented above can be summarized as follows. We supply an experimental proof that the main azimuthal modes (with the indices $m = \pm 1$, no radial nodes) exist only in low fields, below the vortex nucleation field H_n. We also present an observation of a spin mode of the shifted vortex observed by using parallel pumping (the mode 2). This mode splits out from the lowest azimuthal mode (with $m = +1$) and *has a character* described approximately as a superposition of the azimuthal modes with the indices $m = \pm 2$ rotating around the vortex core in the opposite directions. Furthermore, the high-field soft mode (3) localized near the vortex core for parallel pumping was observed. This mode (3) can be approximately described as having a wave vector along the bias field and is stable up to H_a. Finally, we present an observation of the fundamental differences in the field dependence of spin-wave modes excited with *perpendicular* (abrupt change between the SV and MV regions, broad spin-wave response in the MV state) and *parallel* (the spin-wave spectrum more continuously transforms, a single localized mode in the MV state) pumpings.

The authors thank T. Alieva and R. Villar for a critical reading of the paper. This work was supported by Comunidad de Madrid (Contract No. S-505/MAT0194) and Spanish MICINN (Contracts No. MAT2006-07196 and No. Consolider CSD2007-00010). As a part of the European Science Molecular Nanoscience Foundation EUROCORES Programme (Contract No. 05-FONE-FP-010-SPINTRA), work was also supported by funds from the Spanish MEC (Contract No. MAT2006-28183-E) and the EC Sixth Framework Programme under Contract No. ERAS-CT-2003-980409. The authors also acknowledge U.S. NSF (Contract No. NSF-ECCS-0823813) (V.M.), Research Center of Spin Dynamics and Spin-Wave Devices of MEST/KOSEF and the Ikerbasque Science Foundation (K.G.), and Portuguese FCT through the "Ciencia 2007" program (G.N.K.) for support.

*Corresponding author: farkhad.aliev@uam.es
†On leave from Institute of Magnetism National Academy of Sciences of Ukraine, 03142 Kiev, Ukraine

[1] C. C. de Souza Silva, J. V. de Vondel, M. Morelle, and V. V. Moshchalkov, Nature (London) **440**, 651 (2006).
[2] V. M. H. Ruutu, V. B. Eltsov, A. J. Gill, T. W. Kibble, B. Krusius, Yu. G. Makhlin, B. Plaçais, G. E. Volovik, and W. Xu, Nature (London) **382**, 334 (1996).
[3] K. Yu. Guslienko and A. N. Slavin, Phys. Rev. B **72**, 014463 (2005).
[4] B. Van Waeyenberge, A. Puzic, H. Stoll, K. W. Chou, T. Tyliszczak, R. Hertel, M. Fähnle, H. Brückl, K. Rott, G. Reiss, I. Neudecker, D. Weiss, C. H. Back, and G. Schütz, Nature (London) **444**, 461 (2006).
[5] K. Yu. Guslienko, B. A. Ivanov, V. Novosad, Y. Otani, H. Shima, and K. Fukamichi, J. Appl. Phys. **91**, 8037 (2002); K. Yu. Guslienko, X. F. Han, D. J. Keavney, R. Divan, and S. D. Bader, Phys. Rev. Lett. **96**, 067205 (2006).
[6] J. P. Park, P. Eames, D. M. Engebretson, J. Berezovsky, and P. A. Crowell, Phys. Rev. B **67**, 020403(R) (2003).
[7] V. Novosad, F. Y. Fradin, P. E. Roy, K. S. Buchanan, K. Yu. Guslienko, and S. D. Bader, Phys. Rev. B **72**, 024455 (2005).
[8] K. Yu. Guslienko, W. Scholz, R. W. Chantrell, and V. Novosad, Phys. Rev. B **71**, 144407 (2005).
[9] M. Buess, R. Hollinger, T. Haug, K. Perzlmaier, U. Krey, D. Pescia, M. R. Scheinfein, D. Weiss, and C. H. Back, Phys. Rev. Lett. **93**, 077207 (2004).
[10] M. Buess, T. P. J. Knowles, R. Höllinger, T. Haug, U. Krey, D. Weiss, D. Pescia, M. R. Scheinfein, and C. H. Back, Phys. Rev. B **71**, 104415 (2005).
[11] B. A. Ivanov and C. E. Zaspel, Phys. Rev. Lett. **94**, 027205 (2005).
[12] J. P. Park and P. A. Crowell, Phys. Rev. Lett. **95**, 167201 (2005).
[13] X. Zhu, Z. Liu, V. Metlushko, P. Grütter and M. R. Freeman, Phys. Rev. B **71**, 180408(R) (2005).
[14] F. Giesen, J. Podbielski, T. Korn, and D. Grundler, J. Appl. Phys. **97**, 10A712 (2005).
[15] M. J. Pechan, C. Yu, D. Owen, J. Katine, L. Folks, and M. Carey, J. Appl. Phys. **99**, 08C702 (2006).
[16] I. Neudecker, G. Woltersdorf, B. Heinrich, T. Okuno, G. Gubbiotti, and C. H. Back, J. Magn. Magn. Mater. **307**, 148 (2006).
[17] I. Neudecker, K. Perzlmaier, F. Hoffmann, G. Woltersdorf, M. Buess, D. Weiss, and C. H. Back, Phys. Rev. B **73**, 134426 (2006).
[18] K. Rivkin, Wentao Xu, L. E. DeLong, V. V. Metlushko, B. Ilic, and J. B. Ketterson, J. Magn. Magn. Mater. **309**, 317 (2007).
[19] G. N. Kakazei, P. E. Wigen, K. Y. Guslienko, V. Novosad, A. N. Slavin, V. O. Golub, N. A. Lesnik, and Y. Otani, Appl. Phys. Lett. **85**, 443 (2004).
[20] G. N. Kakazei, P. E. Wigen, K. Yu. Guslienko, R. W. Chantrell, and N. A. Lesnik, J. Appl. Phys. **93**, 8418 (2003).
[21] J. F. Sierra, V. V. Pryadun, F. G. Aliev, S. E. Russek, M. García-Hernández, E. Snoeck, and V. V. Metlushko, Appl. Phys. Lett. **93**, 172510 (2008); J. F. Sierra, A. A. Awad, G. N. Kakazei, F. J. Palomares, and F. G. Aliev, IEEE Trans. Magn. **44**, 3063 (2008).
[22] We used the OOMMF code. See http://math/nist.gov/oommf
[23] K. Y. Guslienko, A. N. Slavin, V. Tiberkevich, and S. K. Kim, Phys. Rev. Lett. **101**, 247203 (2008).
[24] G. Gubbiotti, K. Y. Guslienko, A. Andre, C. Bayer, and A. N. Slavin, J. Phys.: Condens. Matter **16**, 7709 (2004).
[25] H. F. Ding, A. K. Schmid, D. Li, K. Y. Guslienko, and S. D. Bader, Phys. Rev. Lett. **94**, 157202 (2005).
[26] See EPAPS Document No. E-PRBMDO-79-042917 for movies of the selected modes shown in Fig. 3, but presented in the time domain. The numbers are correspondingly eigenmode frequencies and the normalized magnetic fields. For more information on EPAPS, see http://www.aip.org/pubservs/epaps.html.
[27] M. R. Fitzsimmons, T. J. Silva, and T. M. Crawford, Phys. Rev. B **73**, 014420 (2006).
[28] S. Kaka, M. R. Pufall, W. H. Rippard, Thomas J. Silva, Stephen E. Russek and Jordan A. Katine, Nature (London) **437**, 389 (2005).